

中国科学院海洋研究所编辑

海洋科学集刊

STUDIA MARINA SINICA

Institute of Oceanology, Chinese Academy of Sciences

47

科学出版社

北京

中国海洋学会 中国海洋学会 中国海洋学会

海洋科学集刊

中国海洋学会 中国海洋学会 中国海洋学会

中国海洋学会 中国海洋学会 中国海洋学会

47

中国海洋学会 中国海洋学会 中国海洋学会

中国海洋学会 中国海洋学会 中国海洋学会

(P-1628.0101)

海洋科学集刊

第47集

中国科学院海洋研究所 编辑

青岛市南海路7号

邮政编码: 266071

科学出版社出版

北京东黄城根北街16号

邮政编码: 100717

<http://www.sciencep.com>

天时彩色印刷有限公司印刷

科学出版社发行 各地新华书店经销

*

2006年4月第一版 开本: 787 × 1092 1/16

2006年4月第一次印刷 印张: 13 1/4 插页: 2

印数: 1—800

字数: 304 000

ISBN 7-03-017163-2



ISBN 7-03-017163-2

定价: 45.00 元

(如有印装质量问题, 我社负责调换〈环伟〉)

9 787030 171634 >

《海洋科学集刊》编辑委员会

THE EDITORIAL BOARD OF *STUDIA MARINA SINICA*

- 主 编** Editor-in-Chief
孙 松 SUN Song
- 副 主 编** Deputy Editors
侯一筠 HOU Yijun 杨红生 YANG Hongsheng
- 顾 问** Advisory Committee
曾呈奎 ZENG Chengkui (C. K. Tseng)
刘瑞玉 LIU Ruiyu (J. Y. Liu)
秦蕴珊 QIN Yunshan
张福绥 ZHANG Fusui
胡敦欣 HU Dunxin
- 编 委** Members (按姓氏笔画为序)
王 凡 WANG Fan 王 雷 WANG Lei
王广策 WANG Guangce 李 军 LI Jun
李安春 LI Anchun 李铁钢 LI Tiegang
李新正 LI Xinzheng 宋金明 SONG Jinming
宋金宝 SONG Jinbao 张国范 ZHANG Guofan
张培军 ZHANG Peijun 范 晓 FAN Xiao
周名江 ZHOU Mingjiang 相建海 XIANG Jianhai
俞志明 YU Zhiming 侯保荣 HOU Baorong
秦 松 QIN Song 阎 军 YAN Jun
黄彦良 HUANG Yanliang
- 主编助理** Editor-Assistant
李新正 LI Xinzheng 宋金明 SONG Jinming
- 编 辑 部** Editorial Office
徐 雯 XU Wen

海洋科学集刊 第 47 集

(2006 年 4 月)

目 录

海浪和潮汐风暴潮耦合过程的数值研究(英文)	
..... 尹宝树 莎日娜 杨德周 等 (1)	
冲绳海槽末次冰期以来千年尺度古海洋演化的沉积记录	
..... 李铁刚 陈金霞 张德玉 等 (16)	
海水养殖环境细菌耐药性的危害	党宏月 宋林生 张志南 (29)
深海极端环境深部生物圈微生物学研究综述	党宏月 李铁刚 曾志刚 等 (41)
冲绳海槽及邻区火山作用与形成演化	黄 朋 李安春 肖尚斌 等 (61)
大洋铁锰结壳成矿环境研究进展	徐兆凯 李安春 蒋富清 (73)
3 000 万年以来南海沉积矿物组成及其地质意义	蒋恒毅 李安春 万世明 (83)
近海海洋石油平台导管架喷涂金属层防腐	李言涛 侯保荣 (95)
胜利油田浅海石油开发区钢铁腐蚀规律	李言涛 侯保荣 (101)
Zn-Al 合金镀层低铬钝化膜的组成和耐蚀性	张 杰 朱松玲 侯保荣 等 (109)
壳聚糖的磺化产物对大鼠血栓和凝血时间的影响	邢荣娥 刘 松 于华华 等 (118)
中国海水经济(养殖)动物种质资源元数据库的概念、内容与体系	
..... 李 军 尤 锋 (124)	
贝类神经内分泌和免疫系统对环境胁迫的响应	高 菲 许 强 陈慕雁 等 (131)
重组斑马鱼 Gli2 蛋白 N 端肽段的表达及纯化	谭训刚 张培军 杜少军 (140)
中国近海珊瑚螺科的补充研究(腹足纲, 骨螺总科)	张素萍 尉 鹏 (149)
中国鲷亚目鱼类地理分布和区系特征	刘 静 田明诚 赵元菀 (158)
中国海洋红藻——御前凹顶藻 <i>Laurencia Omaezakiana</i> Masuda 的形态与结构特征	
..... 丁兰平 黄冰心 曾呈奎 (169)	
中国黄、渤海胶毛藻目(Chaetophorales, Chlorophyta)初探	丁兰平 黄冰心 (176)
中国异枝软骨凹顶藻 <i>Chondrophycus intermedius</i> (Yamada) Garbary et Harper 的	
形态及解剖学	丁兰平 黄冰心 曾呈奎 (182)
底栖生物生物量周年变化动态模型	黄 勃 刘瑞玉 (190)
中国近海皱纹盘鲍不同地理群体的遗传结构与变异研究	
..... 张国范 张喜昌 刘 晓 (194)	

STUDIA MARINA SINICA, No. 47

(April, 2006)

CONTENTS

Numerical Study of Wave-Tide-Surge Coupling Processes	
..... YIN Baoshu, SHA Rina, YANG Dezhou <i>et al.</i> (1)	
Sedimentary Record of Millennial-scale Paleooceanography Evolution since the Last Glaciation in the Okinawa Trough.....	
..... LI Tiegang, CHEN Jinxia, ZHANG Deyu <i>et al.</i> (28)	
Harmfulness of Bacterial Antibiotic Resistance from Maricultural Environments	
..... DANG Hongyue, SONG Linsheng, ZHANG Zhinan (40)	
Microbiological Studies on Subseafloor Deep Biosphere in Deep Sea Extreme Environments	
..... DANG Hongyue, LI Tiegang, ZENG Zhigang <i>et al.</i> (60)	
Magmatism and Evolution of Okinawa Trough and Adjacent Areas	
..... HUANG Peng, LI Anchun, XIAO Shangbin <i>et al.</i> (71)	
Progress in Research on Metallogenic Environment of Ferromanganese Crusts	
..... XU Zhaokai, LI Anchun, JIANG Fuqing (81)	
Terrigenous Mineralogical Component in the Sediments from SCS since 30 Ma and Their Geological Significance	
..... JIANG Hengyi, LI Anchun, WAN Shiming (94)	
Anti-Corrosion by Thermal Spraying Metal Coating for Jacket of Offshore Marine Oil Platform	
..... LI Yantao, HOU Baorong (100)	
Corrosion Behavior of Steel in Offshore Oil Exploitation Area in Shengli Oil Field ...	
..... LI Yantao, HOU Baorong (108)	
Composition and Anti-Corrosion Performance of Chromate Conversion Film on Hot Dip Zn-Al Alloy Coating	
..... ZHANG Jie, ZHU Songling, HOU Baorong <i>et al.</i> (117)	
Effect of Chitosan Sulfate on Thrombus Formation and Cruor Time in Mice	
..... XING Rong, LIU Song, YU Huahua <i>et al.</i> (123)	
The Concept, Content and System of Genetic Resources Metadatabase on China Marine Economically Valuable(Cultivated) Animals	
..... LI Jun, YOU Feng (129)	
Stress-induced Neuroendocrine and Immune Responses in Mollusks : a Review	
..... GAO Fei, XU Qiang, CHEN Muyan <i>et al.</i> (138)	
Expression and Purification of N-Terminal Partial Protein of Recombination Zebrafish Gli2	
..... TAN Xungang, ZHANG Peijun, DU Shaojun (148)	

- Study on the Coralliophilidae Supplement from China(Gastropoda: Muricacea)
 ZHANG Suping, WEI Peng (156)
- The Geographical Distribution and Fauna Characteristics of the Blennioid Fishes from
 Chinese Waters LIU Jing, TIAN Mingcheng, ZHAO Yuanjun (168)
- The Morphology and Anatomy on *Laurencia Omaezakiana* Masuda from the Coast of
 Yellow Sea, China DING Lanping, HUANG Bingxin, C. K. Tseng (175)
- The Taxonomic Study on Order Chaetophorales(Chlorophyta)from Yellow-Bohai Sea of
 China DING Lanping, HUANG Bingxin (181)
- The Morphology and Anatomy of *Chondrophycus Intermedius*(Yamada) Garbary et
 Harper from China Coasts DING Lanping, HUANG Bingxin, C. K. Tseng (189)
- Macrobenthic Biomass Annual Dynamic Models in Jiaozhou Bay
 HUANG Bo, LIU Ruiyu (193)
- The Genetic Structure and Variation of Wild Populations of Pacific Abalone, *Haliotis*
Discus Hannai Ino in China Seas
 ZHANG Guofan, ZHANG Xichang, LIU Xiao (205)

Numerical Study of Wave-Tide-Surge Coupling Processes^{*}

YIN Baoshu¹ SHA Rina^{1,2} YANG Dezhou¹ CHENG Minghua¹

(¹ Institute of Oceanology, Chinese Academy of Sciences, Qingdao 266071)

(² Graduate School, Chinese Academy of Sciences, Beijing 100039)

Risk assessment of storm surge and wave hazards in the Huanghe Delta coastal area of the Bohai Sea requires accurate prediction of storm surge and wave hazards. So this study is aimed at establishing a coastal high-resolution ($2' \times 2'$) two-way coupled wave-tide-surge model, including three main physical mechanisms. The model was used for comparisons and analysis of simulated and measured wave heights and sea level in two moderate storm cases in the Huanghe Delta coastal area. We show that the effects of different physical mechanisms on wave heights are mainly determined by wave-current interaction by radiation stress in the wave energy equation. Wave-age dependent surface wind stress and radiation stress mechanisms in the coupling wave-tide-surge interaction have positive impact on sea level, and wave-current interaction bottom stress mechanism show negative impact on sea level. The comprehensive effects of three main physical mechanisms show positive net impact on sea level and increase it by as much as 25 cm. We show that the wave heights and sea levels simulated by the coupled wave-tide-surge model agree better with the measured values compared to uncoupled model results, particularly for peak storm conditions.

I. INTRODUCTION

As wind generates waves and storm surges, their generation is closely related. The strong nonlinear interactions between tides and storm surges in shallow water result in important interactions between waves and tide-surge motions. This study showed that the coupling of waves and tide-surge motions is driven by several mechanisms where in waves and the mean flow, or the water level associated with the tide and surge, interact with each component of the total motion affecting the other motions. These mechanisms mainly include the wave-state dependent surface wind stress, the wave-current interaction bottom stress, and the radiation stress. In the past ten years, several studies (Mastenbroek *et al.*, 1993; Davies *et al.*, 1994; Zhang

* Corresponding author: Dr YIN Baoshu, E-mail: bsyin@ms.qdio.ac.cn; Fax: (0532)82898612

收稿日期: 2005 年 7 月 26 日。

et al., 1996; Jin *et al.* 1998; Yin *et al.*, 2001) considered wave and tide-surge interaction mechanisms. However, because of the large spatial resolutions used in these studies, the effects of radiation stress were ignored or poorly simulated and only some individual coupling mechanisms were studied or some studies considered only one-way coupling. Lin *et al.* (2003) made a preliminary study on the impact of radiation stress using two-way coupling model. In this work high-spatial resolution and a two-way coupled wave-surge interaction numerical model, are used to study the net effects of several physical mechanisms driving wave heights and sea level.

This study is focused on wave-tide-surge interactions in the coastal region, specifically the Huanghe Delta area of the Bohai Sea. High quality models are implemented on waves, tides and surges on a fine-resolution grid. The coupling mechanisms considered are wave radiation stress, wave-current interaction bottom stress and wave-state dependent surface wind stress. For moderately high wind and current conditions, coupled model simulation results are compared with synchronic in situ measurements of waves, currents and elevation, and finally the net impacts are studied to give quantitative estimates and appraisal of the wave-surge coupling interaction. This is extremely important for risks assessment of storm surge and wave hazards in the Huanghe Delta coastal area, marine environmental forecasts, ocean engineering design etc. In the Bohai Sea.

II. COUPLED WAVE-TIDE-SURGE MODEL

The coupled wave-tide-surge interaction numerical model is composed of an advanced shallow water wave model and a two-dimensional tide-surge model. Two-way interactions between waves and tide-surge motions are studied on the basis of wave-state dependent surface stress, wave-current interaction bottom stress and radiation stress mechanisms.

(1) Wave Model

The third generation shallow water wave model YWE-WAM used in this study is based on the wave action balance equation, with most of the source functions taken directly from the standard WAM model of Komen *et al.* (1994). An explicit representation of the energy dissipation caused by depth-limited wave breaking in shallow water is taken into account. The basic equations are

$$\frac{\partial N}{\partial t} + \nabla [(\vec{C}_g + \vec{u})N] + \frac{\partial}{\partial \sigma} [C_\sigma N] + \frac{\partial}{\partial \theta} (c_\theta N) = \frac{S}{\sigma} \quad (1)$$

$$N = N(\sigma, \theta, \vec{x}, t) = \frac{F(\sigma, \theta, \vec{x}, t)}{\sigma} \quad (2)$$

$$C_g = \frac{1}{2} \left(1 + \frac{2kd}{\sinh 2kd} \right) \frac{\sigma}{k}; \quad C_\theta = -\frac{1}{k} \left(\frac{\partial \sigma}{\partial d} \frac{\partial d}{\partial m} - \vec{k} \cdot \frac{\partial \vec{u}}{\partial m} \right) \quad (3)$$

$$C_\sigma = \frac{\partial \sigma}{\partial d} \left(\frac{\partial d}{\partial t} + \vec{u} \cdot \nabla d \right) - C_g \vec{k} \cdot \frac{\partial \vec{u}}{\partial s}. \quad (4)$$

where $F(\sigma, \theta)$ is the spectral density, d , \vec{k} , \vec{u} are water depth, wave number vector, velocity vector, s is the space coordinate in the propagation direction, θ , the two-dimensional space gradient is ∇ , and m is the spatial coordinate perpendicular to the propagation direction, θ . The formulations for propagation speed C_g , C_σ and C_θ detailedly considers the effect of varying depth and currents on wave propagation. Source functions are given by: $S = S_{in} + S_{nl} + S_{dis} + S_{bot} + S_{dbs}$, including wind input, nonlinear interactions, white-capping dissipation, bottom friction and depth-limited wave breaking dissipation. A detailed description of the model is given by Yin *et al* (1996).

(2) Tide-Surge Model

A two-dimensional numerical tide-surge model with ADI (Alternative Direction Implicit) difference scheme and radiation stress is used. The mass equation is

$$\frac{\partial \zeta}{\partial t} + \frac{\partial (Du)}{\partial x} + \frac{\partial (Dv)}{\partial y} = 0 \quad (5)$$

the momentum equations are

$$\frac{\partial u}{\partial t} + u \frac{\partial u}{\partial x} + v \frac{\partial u}{\partial y} - fv = -g \frac{\partial \zeta}{\partial x} - \frac{1}{\rho_w} \frac{\partial p_a}{\partial x} + \frac{1}{\rho_w D} \left(\tau_x - \tau_{bx} - \frac{\partial s_{xx}}{\partial x} - \frac{\partial s_{xy}}{\partial y} \right) + A \left(\frac{\partial^2 u}{\partial x^2} + \frac{\partial^2 u}{\partial y^2} \right) \quad (6)$$

$$\frac{\partial v}{\partial t} + u \frac{\partial v}{\partial x} + v \frac{\partial v}{\partial y} + fu = -g \frac{\partial \zeta}{\partial y} - \frac{1}{\rho_w} \frac{\partial p_a}{\partial y} + \frac{1}{\rho_w D} \left(\tau_y - \tau_{by} - \frac{\partial s_{yx}}{\partial x} - \frac{\partial s_{yy}}{\partial y} \right) + A \left(\frac{\partial^2 v}{\partial x^2} + \frac{\partial^2 v}{\partial y^2} \right) \quad (7)$$

where u and v are components of the depth-averaged velocity in the eastward and northward directions, respectively; t is the time, f is the Coriolis parameter; A is the horizontal eddy viscosity; g is gravitational acceleration; ρ_w is the density of sea water; D is the total depth ($= d + \zeta$; mean water depth + surface elevation); s_{xx} , s_{xy} , s_{yx} and s_{yy} are components of the radiation stress tensor; p_a is the atmospheric pressure $\vec{\tau}_s = (\tau_x, \tau_y)$ is the surface wind stress; and $\vec{\tau}_b = (\tau_{bx}, \tau_{by})$ is the bottom stress. Surface wind stress is generally assumed to take the form;

$$\vec{\tau}_s = \rho_a C_d \left| \vec{w}_{10} \right| \vec{w}_{10} \quad (8)$$

where ρ_a is the air density; C_d , is the surface aerodynamic drag coefficient and \vec{w}_{10} denotes wind velocity vector at 10m reference height. In this study, a conventional approach C_d , following Hsu(1986), is assumed to takes the form:

$$C_d = \lambda \left\{ \frac{0.4}{14.56 - 2 \ln \left| \vec{w}_{10} \right|} \right\}^2 \quad (9)$$

where λ is an adjustable coefficient depending on different weather conditions (~ 1.1 for typhoons, ~ 1.0 for extra-tropical systems). For considering wave-dependent state surface wind stress, a wave-age dependent C_d formulation would assume the functional dependence of the HEXOS relation of Smith (1992), but here we take a more convenient expression following Donelan *et al.* (1993):

$$z_p = 3.7 \times 10^{-5} \frac{w_{10}^2}{g} \left(\frac{c_p}{w_{10}} \right)^{-0.9} \quad (10)$$

C_d can be obtained by

$$C_d = \left[\frac{\kappa}{\ln 10 - \ln z_0} \right]^2 \quad (11)$$

where c_p is phase velocity of spectral peak and κ is Karman constant ($=0.40$).

When we do not consider wave-current interactions, bottom stress is assumed to be

$$\vec{\tau}_b = \rho_w \gamma |\vec{u}| \vec{u}, \gamma = \frac{ng}{c_z^2} \quad (12)$$

where c_z is the Chezy-Manning coefficient and \vec{u} is the current velocity vector.

According to the wave-current interaction model of Grant and Madsen(1979), in the form published by Signell *et al*(1990), a collinear flow implies that the total bed shear stress is given by

$$\tau_t = \tau_c + \tau_w \quad (13)$$

where τ_c is an instantaneous current shear stress and τ_w is the maximum wave bed stress, as given by

$$\tau_w = \frac{1}{2} \rho f_w |U_0|^2 \quad (14)$$

where U_0 is the maximum near-bed wave orbital velocity, and f_w is the wave friction factor. The near-bed wave orbital velocity is given by

$$U_0 = \frac{a_w \sigma}{\sinh kh} \quad (15)$$

where a_w is the wave amplitude, σ is wave frequency, and k is the wave number determined from the linear dispersion relation

$$\sigma^2 = (gk) \tanh(kh). \quad (16)$$

The wave friction factor f_w can be readily computed from the semi-empirical expression of Jonsson and Carlsen(1976), based on laboratory observations, This implies

$$\frac{1}{4\sqrt{f_w}} + \lg\left(\frac{1}{4\sqrt{f_w}}\right) = -0.08 + \lg\left(\frac{A_b}{k_b}\right) \quad (17)$$

where $k_b = 30z_0$, and z_0 is the bottom roughness length and $A_b = U_0/\sigma$.

If we assume that the current does not influence the wave field, the wave friction velocity is given by

$$U_{*w} = \left(\frac{\tau_w}{\rho} \right)^{1/2}. \quad (18)$$

At initial time $t=0$, an initial current friction factor f_c , excluding wind wave turbulence, is determined from

$$f_c = 2 \left[\frac{0.4}{\ln(30z_r/k_{bc})} \right]^2 \quad (19)$$

with k_{bc} taken as the Nikuradse roughness $k_{bc} = k_b = 30z_0$, with z_r taken as 100 cm above the bed. Once f_c is determined, U_{*c} can be readily computed from

$$U_{*c} = \left(\frac{\tau_c}{\rho} \right)^{1/2} \quad (20)$$

where $\tau_c = \sqrt{F_B^2 + G_B^2}$ and F_B and G_B are given as

$$F_B = \frac{1}{2} f_c \rho u (u^2 + v^2)^{1/2} \quad (21)$$

$$G_B = \frac{1}{2} f_c \rho v (u^2 + v^2)^{1/2}. \quad (22)$$

The combined friction velocity U_{*cw} for waves and currents is given by

$$U_{*cw} = (U_{*c}^2 + U_{*w}^2)^{1/2}. \quad (23)$$

The apparent bottom roughness k_{bc} felt by the current due to the presence of waves is given by

$$k_{bc} = k_b \left(C_1 \frac{U_{*cw} A_b}{U_w k_b} \right)^\beta \quad (24)$$

with $C_1 = 24.0$ from Grant and Madsen (1979), and

$$\beta = 1 - \frac{U_{*c}}{U_{*cw}}. \quad (25)$$

The value for k_{bc} is then used at the next time step to determine f_c , and hence the bed stress due to the wave field and the time-evolving viscosity field may be estimated as

$$\vec{\tau}_c = \frac{1}{2} \rho f_c |\vec{u}|^2 \vec{u} \quad (26)$$

The radiation stress components are given by

$$s_{xx} = \rho g \int_0^\infty \int_0^{2\pi} \left[\left(n - \frac{1}{2} \right) + n \cos^2 \theta \right] F(\sigma, \theta) d\sigma d\theta \quad (27)$$

$$s_{xy} = s_{yx} = \rho g \int_0^\infty \int_0^{2\pi} (n \sin \theta \cos \theta) F(\sigma, \theta) d\sigma d\theta \quad (28)$$

$$s_{yy} = \rho g \int_0^\infty \int_0^{2\pi} \left[\left(n - \frac{1}{2} \right) + n \sin^2 \theta \right] F(\sigma, \theta) d\sigma d\theta \quad (29)$$

where $n = \frac{1}{2} \left(1 + \frac{2kd}{\sinh 2kd} \right)$. Given $F(\sigma, \theta)$ by a wave model, radiation stress can therefore be obtained.

(3) Initial and Boundary Conditions

Initial conditions are that currents and surface elevation are zero,

$$\zeta = u = v = 0 \quad (30)$$

Lateral boundary conditions are assumed zero for flow normal to the solid boundary and along the open boundary,

$$\zeta = \frac{P_b - P_o}{\rho g} + \sum f_i H_i \cos [\omega_i t + (\nu + u)_i - g_i] \quad (31)$$

where P_o and P_b are the values for atmospheric pressure outside a storm and at the open boundary, respectively; ρ is the density of seawater, g is gravitational acceleration; ω_i is the radian frequency; harmonic constants H_i and g_i are the amplitudes and phase angles of each tidal con-

stituent; f_i is the nodal factor of each tidal constituent; t is the time; $(\nu + u)_i$ is the initial phase and u_i is the nodal correction angle. The ten constituents in standard notation are K_1 , O_1 , P_1 , Q_1 , M_2 , S_2 , N_2 , K_2 , S_a , S_{sa} .

(4) The Coupling Procedure

Implementation of the coupling between wave and tide-surge models followed the procedure below.

- Prior to the coupling, the two models are initialized separately. Thus, the wave model is warmed up for 12 h, and the tide-surge model, for 4 days. Initialization is performed in a manner permitting the synchronized coupling of the two models.
- The wave model is run (in 3 minute time-steps) for 5 time-steps using the computed change of water depth (mean water depth plus tide-surge elevation) and inhomogeneous and unsteady currents from the two-dimensional tide-surge model to obtain related wave parameters, such as wave spectrum.
- The wave-age dependent surface wind stress, radiation stress and wave-current bottom stress are calculated using the wave spectrum and passed back to the tide-surge model.
- The two-dimensional tide-surge model is run (15 minute time-steps) using the calculated radiation stress, surface wind stress and bottom stress. This gives newly computed elevations and currents which are passed back to the wave model to repeat the sequence of the computations.

During the simulation, computed results of interest, for example, the significant wave heights, the mean wave periods, the directional wave spectrum, water surface elevations and current velocities, with and without the inclusion of waves and tide-surge interactions can be output by the wave model and tide-surge model, as described.

III. NUMERICAL STUDY OF WAVE-TIDE-SURGE COUPLING INTERACTION IN THE HUANGHE DELTA COASTAL AREA

The Huanghe Delta coastal area located in the southwest region of the Bohai Sea has great strategic importance because it is the most important oil production area of the Shengli Oilfield. The fine-resolution grid area shown in Fig. 1 is the Huanghe Delta coastal area, which is the focus of this study. This area is characterized by relatively big waves and strong set-up due to its shallow water depth (generally less than 12 m) and long fetch, and presents a challenging problem for offshore design for prediction, particularly in severe storms with extreme wind and waves conditions. Accurate forecasts of waves and sea level are very important for the safety of offshore personnel and property and for risks assessment. This study is aimed at determining, the comprehensive effects of different coupling interaction physical mechanisms on wave heights and sea level, in the context of a wave-surge coupling interaction model and gives a quantitative estimate and comprehensive appraisal of coupling interaction. A secondary objective is to offer a feasible analysis for the operational adoption of a coupled wave-surge model to forecast

waves and storm surges hazards and lay the foundation of risks assessment of storm surge and wave hazards in a coastal region such as the Huanghe Delta area.

(1) Case Descriptions

A storm cases occurred on 22 ~ 25 April 1998 and one on 1-2 April 1999, where synchronized in situ measured wave, current and elevation data were collected from a buoy at $38^{\circ}13'N$, $118^{\circ}19'E$ (shown in Fig. 1). The observed wind fields were prepared by Ocean University of China. The wave model and tidesurge model were implemented on the $2' \times 2'$ grid covering the entire Bohai Sea. The comprehensive effects of different physical mechanisms on wave heights and sea level in the Huanghe Delta coastal area (specifically, $118^{\circ}24' \sim 119^{\circ}24'E$, $37^{\circ}48' \sim 38^{\circ}14'N$) can be analyzed by comparing results from uncoupled and coupled model simulations synchronized in situ measurements of wave, current and elevation data.

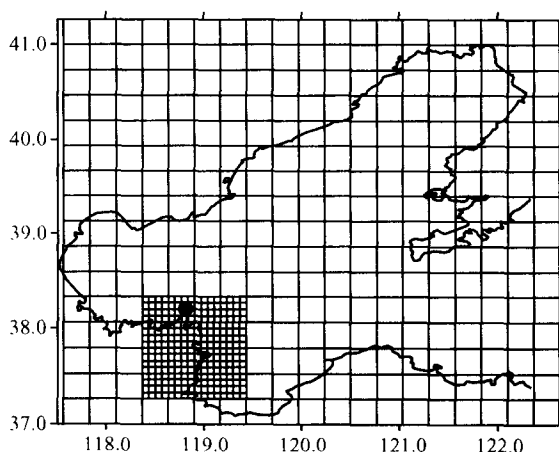


Fig. 1 The Bohai and Huanghe Delta coastal area, with buoy location

• The fine-mesh grid in Fig. 1 is shown as $4'$ to avoid blackening the figure. The actual resolution is $2'$ in the computations for the entire Bohai Sea.

(2) Impact of radiation stress on wave heights and sea level

The coupled wave-tide-surge model used to investigate the influence of radiation stress in wave-tide-surge interactions only includes a radiation stress mechanism. Fig. 2 ~ 5 compares simulated and measured wave heights and sea level for the two cases, at the buoy. From Fig. 2 ~ 3, the wave heights simulated by coupled wave-tide-surge model show overall improvement, particularly for the second storm case (1 ~ 2 April 1999), compared to those simulated by the uncoupled wave model at maximum wave heights values. Moreover, Fig. 4 ~ 5 show that the sea level simulated by coupled wave-tide-surge model is improved compared to those simulated by the uncoupled tide-surge model. The improvement is more clearly evident at the maximum set-up values, and in very good agreement with the measured data. Radiation stress can increase the wave heights by as much as 67 cm, and sea level, by as much as 50 cm. This indicates the impact of radiation stress is positive.

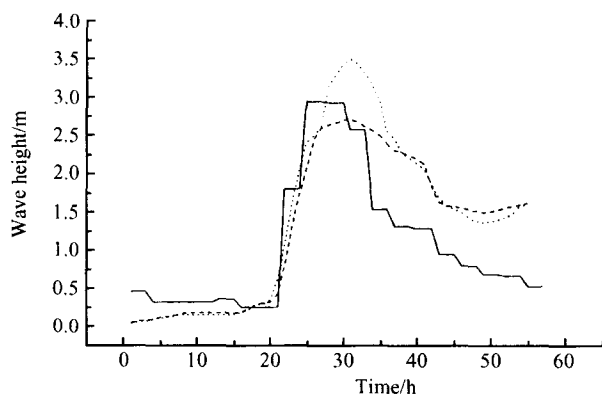


Fig. 2 Comparisons of simulated and measured wave heights for the 20UTC 22 April 1998-02UTC 25 April 1998 storms

Measured data—; uncoupled wave model---; coupled wave-tide-surge model(radiation stress mechanism)....

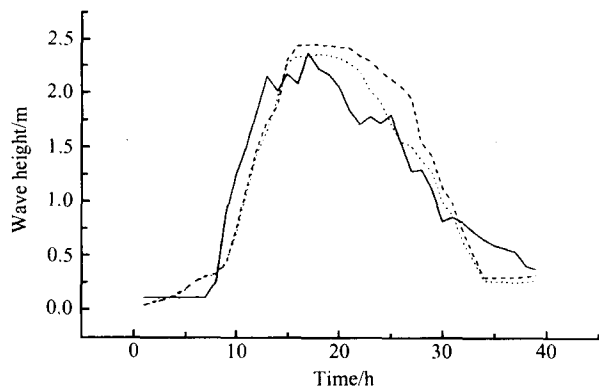


Fig. 3 As in Fig. 2, for the 00UTC 01 April 1999-14UTC 02 April 1999 storms

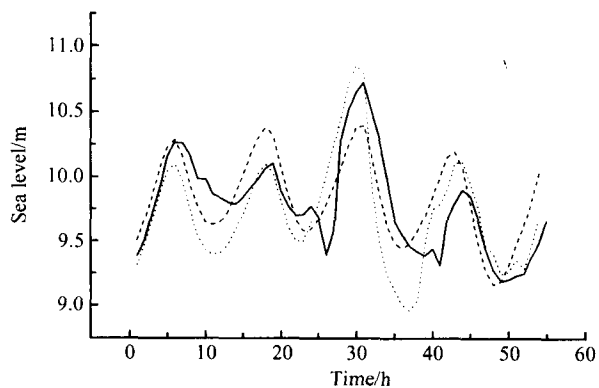


Fig. 4 Comparisons of simulated and measured sea level for the 20UTC 22 April 1998-02UTC 25 April 1998 storms

Measured data—; uncoupled tide-surge model---; coupled wave-tide-surge model(radiation stress mechanisms)....

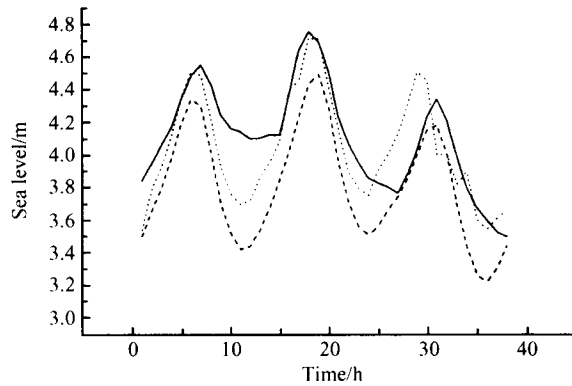


Fig. 5 As in Fig. 4, for the 00UTC 01 April 1999-14UTC 02 April 1999 storms

(3) Impact of wave-current interaction bottom stress on wave heights and sea level

To investigate the influence of wave-current interaction bottom stress in wave-tide-surge interactions, the coupled wave-tide-surge model used ouag includes the wave-current interaction bottom stress mechanism. Fig. 6 ~ 7 show comparisons of simulated and measured sea level for the two cases, at the buoy. It follows that wave height estimates (Figures not shown) are almost the same as those in Fig. 2 ~ 3. Fig. 6 ~ 7 show that estimated sea level obtained from the coupled wave-current model are smaller than the results obtained from the uncoupled tide-surge model. These effects can be understood in terms of the wave-bottom effects. The effects of waves on the current bottom boundary layer is significant, and in fact the bottom stress is increased due to the wave-current interaction. Therefore, the coupled wave-current model is an important consideration because of the physical factors that it represents. Moreover, our results imply that the coupled wave-current model should be the basis for simulating the current velocity and sea level in the nearshore region. The results also showed that the impact of wave-current interaction bottom stress is negative.

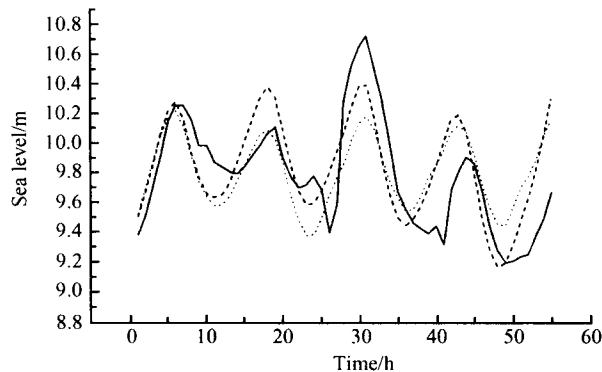


Fig. 6 Comparisons of simulated and measured sea level for the 20UTC 22 April 1998-02UTC 25 April 1998 storms

Measured data—; uncoupled tide-surge model---; coupled wave-tide-surge model (wave-current interaction bottom stress mechanism)....

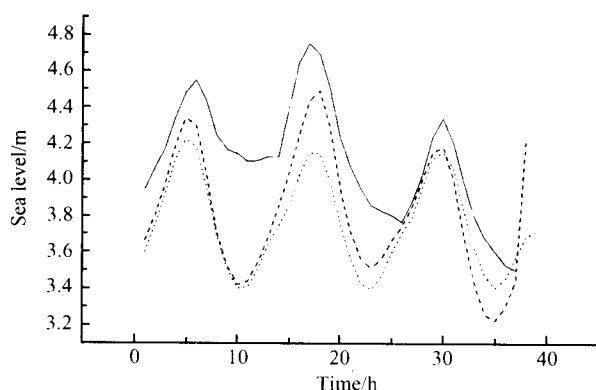


Fig. 7 As in Fig. 6, for the 00UTC 01 April 1999-14UTC 02 April 1999 storms

(4) Impact of wave-age dependent surface wind stress on wave heights and sea level

To investigate the influence of wave-age dependent surface wind stress in wave-tide-surge interactions, the coupled wave-tide-surge model includes the wave-age dependent mechanism. Fig. 8 ~ 9 show comparisons of simulated and measured sea level for the two cases, at the buoy. Again, almost same wave height estimates (Figures not shown) as the Fig. 2 ~ 3 were obtained. Moreover, Fig. 8 ~ 9 show that the sea level simulated by coupled model is improved compared to sea level simulated by the uncoupled tide-surge model. The improvement is more clearly evident at the maximum set-up values, and in very good agreement with the measured data. These effects can be understood because young wind waves are usually steeper than old wind waves and therefore extract more momentum from the air flow. As a result, airflow over young wind sea is rougher than over old wind sea, and wave-age dependent surface wind stress driving tide-surge motion is generally increased compared to traditional surface wind stress. Wave-age dependent surface wind stress can increase the sea level by as much as 25 cm, which indicates the impact of wave-state dependent surface wind stress is positive.

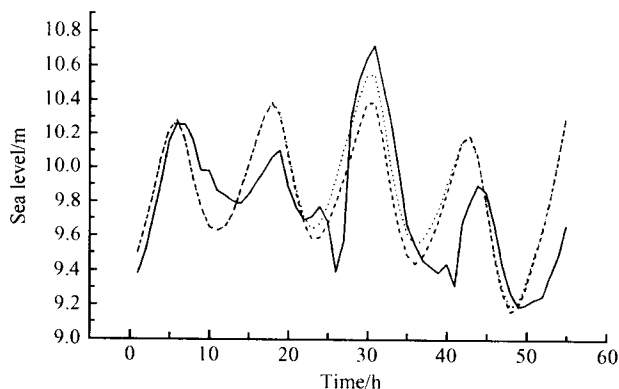


Fig. 8 Comparisons of simulated and measured sea level for the 20UTC 22 April 1998-02UTC 25 April 1998 storms

Measured data—; uncoupled tide-surge model---; coupled wave-tide-surge model(wave-age dependent surface wind stress mechanism)....